THE JOURNAL OF BIOLOGICAL CHEMISTRY VOL. 281, NO. 24, pp. 16482–16492, June 16, 2006
Printed in the U.S.A.

Protein-tyrosine Phosphatase (PTP) Wedge Domain Peptides

*A NOVEL APPROACH FOR INHIBITION OF PTP FUNCTION AND AUGMENTATION OF PROTEIN-TYROSINE KINASE FUNCTION**

Received for publication, April 3, 2006, Published, JBC Papers in Press, April 12, 2006, DOI 10.1074/jbc.M603131200

Youmei Xie[‡], Stephen M. Massa[§¶], Sonya E. Ensslen-Craig[‖], Denice L. Major[‖], Tao Yang[‡], Michelle A. Tisi[§], Vicki D. Derevyanny[‡], William O. Runge[‡], Brijesh P. Mehta[‡], Laura A. Moore[‡], Susann M. Brady-Kalnay[¶1], and Frank M. Longo[‡2]

From the [‡]Department of Neurology, University of North Carolina, Chapel Hill, North Carolina 27599, [§]Department of Neurology and [¶]Laboratory for Computational Neurochemistry and Drug Discovery, San Francisco Veterans Affairs Medical Center and Dept. of Neurology, University of California, San Francisco, San Francisco, California 94121, and [‖]Departments of Neurosciences and Molecular Biology and Microbiology, Case Western Reserve University, Cleveland, Ohio 44106

Inhibition of protein-tyrosine phosphatases (PTPs) counterbalancing protein-tyrosine kinases (PTKs) offers a strategy for augmenting PTK actions. Conservation of PTP catalytic sites limits development of specific PTP inhibitors. A number of receptor PTPs, including the leukocyte common antigen-related (LAR) receptor and PTPμ, contain a wedge-shaped helix-loop-helix located near the first catalytic domain. Helix-loop-helix domains in other proteins demonstrate homophilic binding and inhibit function; therefore, we tested the hypothesis that LAR wedge domain peptides would exhibit homophilic binding, bind to LAR, and inhibit LAR function. Fluorescent beads coated with LAR or PTPμ wedge peptides demonstrated PTP-specific homophilic binding, and LAR wedge peptide-coated beads precipitated LAR protein. Administration of LAR wedge Tat peptide to PC12 cells resulted in increased proliferation, decreased cell death, increased neurite outgrowth, and augmented Trk PTK-mediated responses to nerve growth factor (NGF), a phenotype matching that found in PC12 cells with reduced LAR levels. PTPμ wedge Tat peptide had no effect on PC12 cells but blocked the PTPμ-dependent phenotype of neurite outgrowth of retinal ganglion neurons on a PTPμ substrate, whereas LAR wedge peptide had no effect. The survival- and neurite-promoting effect of the LAR wedge peptide was blocked by the Trk inhibitor K252a, and reciprocal co-immunoprecipitation demonstrated LAR/TrkA association. The addition of LAR wedge peptide inhibited LAR co-immunoprecipitation with TrkA, augmented NGF-induced activation of TrkA, ERK, and AKT, and in the absence of exogenous NGF, induced activation of TrkA, ERK, and AKT. PTP wedge domain peptides provide a unique PTP inhibition strategy and offer a novel approach for augmenting PTK function.

Within intracellular signaling networks, protein-tyrosine kinases (PTKs)[3] can be counterbalanced by protein-tyrosine phosphatases (PTPs) (1–4). Trk-family neurotrophin PTK receptors undergo ligand-induced tyrosine transphosphorylation and downstream activation of mitogen-activated protein kinase and phosphatidylinositol 3-kinase/AKT signaling pathways (5, 6). A fundamental area of Trk signaling that remains to be investigated is the identification of the PTPs that directly or indirectly associate with Trk receptors and regulate their signaling.

The leukocyte common antigen-related (LAR) receptor is a prototypical receptor PTP containing tandem catalytic domains (D1 and D2) in its cytoplasmic region with D1, constituting the primary catalytic site, and D2, conferring regulatory function (7). LAR is expressed by neurons and regulates neuronal survival and neurite outgrowth (2, 8–14). The physiological ligand(s) for LAR in mammalian systems is unknown, although a LAR ectodomain isoform binds LAR homophilically and promotes neurite outgrowth (15). The LAR enzymatic substrates within neurons remain to be established. Several lines of evidence point to LAR as a candidate PTP modulating Trk phosphorylation. First, LAR and Trk are co-expressed in multiple neuronal populations (16); second, LAR associates with caveolin, a component of TrkA signaling complexes (17, 18); finally, antisense-mediated down-regulation of LAR in PC12 cells leads to enhanced nerve growth factor (NGF)/TrkA-induced differentiation (19).

The conserved nature of PTP catalytic sites has limited development of PTP-specific catalytic site inhibitors (20). LAR is one of a subgroup of receptor PTPs (RPTPs), including PTPμ, RPTPα, PTPδ, PTPσ, and CD45, that contain a helix-loop-helix (HLH), wedge-shaped sequence located between the membrane proximal region and the D1 catalytic domain (21, 22). Although functions of the LAR HLH wedge domain remain unknown, HLH domains in other types of proteins mediate homophilic or heterophilic binding (23–25), and in some cases this binding achieves a potent inhibitory effect (26, 27). Application of synthetic peptides resembling potential protein-protein interaction sites, including the c-Myc HLH domain (28), has served as a powerful tool for development of novel strategies to inhibit protein function (29). Despite the absence of knowledge regarding LAR wedge domain binding targets or function, we tested the empiric possibility that a synthetic peptide resembling this domain would demonstrate homophilic binding, bind to full-length LAR, and induce a LAR-deficient phenotype consistent with inhibition of LAR function. We previously established that antisense-induced down-regulation of LAR in PC12 cells induces a phenotype consisting of increased proliferation in serum-containing medium, decreased death, and increased neurite outgrowth in serum-free

* This research was supported in part by National Institutes of Health Grants R01-AG09873 (to F. M. L.) and R01-EY12251 (to S. B.-K.) and by the Veterans Administration (to F. M. L. and S. M. M.). The costs of publication of this article were defrayed in part by the payment of page charges. This article must therefore be hereby marked "*advertisement*" in accordance with 18 U.S.C. Section 1734 solely to indicate this fact.

[1] Supported by NEI, National Institutes of Health Core Grant PO-EY11373 (to the Visual Sciences Research Center of Case Western Reserve University).

[2] To whom correspondence should be addressed: Dept. of Neurology and Neurological Sciences, Stanford University, 300 Pasteur Dr., Stanford, CA 94305. Tel.: 650-725-6673; Fax: 650-498-4579; E-mail: longo@stanford.edu.

[3] The abbreviations used are: PTK, protein-tyrosine kinase; PTP, protein-tyrosine phosphatase; RPTP, receptor PTP; ERK, extracellular signal-regulated kinase; LAR, leukocyte common antigen; NGF, nerve growth factor; HLH, helix-loop-helix; BSA, bovine serum albumin; DMEM, Dulbecco's modified Eagle's medium; HS, horse serum; FBS, fetal bovine serum; Bis-Tris, 2-[bis(2-hydroxyethyl)amino]-2-(hydroxymethyl)propane-1,3-diol; BrdUrd, bromodeoxyuridine; TUNEL, terminal dUTP nick-end labeling; DAPI, 4′,6-diamidino-2-phenylindole; EGF, epidermal growth factor.

medium and enhanced neurite outgrowth in response to NGF stimulation (19). We hypothesized that LAR wedge peptide treatment of PC12 cells would induce a similar phenotype including augmented signaling via the TrkA PTK receptor. The finding that LAR wedge peptides are capable of inhibiting LAR function would suggest novel approaches for inhibition of PTP-dependent functions and for augmentation of neurotrophin signaling.

EXPERIMENTAL PROCEDURES

Peptides—Peptides containing the residues shown in Fig. 1 were synthesized by Genemed Synthesis Inc. (South San Francisco, CA) in the amide form. Peptides were purified by high performance liquid chromatography, and amino acid content was verified by quantitative amino acid analysis. Peptides were synthesized to include a membrane-penetrant Tat-derived sequence at either the C or N terminus, a well established strategy for promoting cellular uptake of protein or synthetic peptides (30).

Microsphere Homophilic Binding Assay—Peptides or bovine serum albumin (BSA) in solutions of 300 μg/ml were each linked to microspheres (Polysciences, Warrington, PA) using the manufacturer's recommended protocol. LAR wedge domain (WLAR-Tat) and scrambled LAR wedge (SLAR-Tat) peptides or BSA were linked to Fluoresbrite Carboxylate NYO (red fluorescing) 1.75-μm microspheres. WPTPμ-Tat and SPTPμ-Tat wedge peptides were linked to Fluoresbrite Carboxylate BB (blue fluorescing) 1.75-μm microspheres. After linkage, microspheres were blocked with 0.25 M ethanolamine for 30 min at room temperature and then with BSA (10 mg/ml) in borate buffer for an additional 30 min. After blocking, microspheres were washed 3 times with phosphate-buffered saline, suspended in 50 μl of phosphate-buffered saline, and then incubated in 96-well plates at room temperature for 1 h on a rotary shaker. 10-μl aliquots were removed and examined on microscope slides using fluorescence microscopy at wavelengths of 360 nM (blue) and 590 nM (red).

Cell Culture—PC12 cells (provided by William C. Mobley, Stanford University (31)) were propagated in Dulbecco's modified Eagle's medium (DMEM) with 4.5 g/liter glucose (Invitrogen) supplemented with 10% heat-inactivated horse serum (HS), 5% fetal bovine serum (FBS), 100 units/ml penicillin, and 100 μg/ml streptomycin. The PC12 cells used in the present study remain attached to tissue culture plastic as a dispersed monolayer (31). Cells were cultured in a humidified incubator with an atmosphere of 5% CO_2, 95% air at 37 °C. LAR-deficient PC12 cells stably transfected with the pMEP4b LAR antisense construct regulated by the metallothionine promoter (32), and control PC12 cells stably transfected with a pMEP4b null construct have been described previously (19).

Pull-down Assays—Pull-down assays were conducted as previously described (15). PC12 cells were grown to 80% confluence in 10% HS and 5% FBS and then lysed at 4 °C in lysis buffer (20 mM Tris-HCl, pH 7.5, 137 mM NaCl, 1% Nonidet P-40, 10% glycerol, 500 μM sodium orthovanadate, 1 mM phenylmethylsulfonyl fluoride, 10 μg/ml aprotinin) for 30 min. Lysates were centrifuged at 14,000 × *g* at 4 °C for 20 min, and the protein concentrations of the supernatant were determined by the BCA method (Pierce). Lysates aliquots of ~700 μl were incubated for 1 h at room temperature with WLAR-Tat or SLAR-Tat (30 μg) synthesized to include a poly-His tag at the C terminus (WLAR-Tat-H, SLAR-Tat-H). After the addition of 100 μl of Talon Superflow metal affinity resin (Clontech, Palo Alto, CA), lysate mixtures were incubated by end-over-end rotation overnight at 4 °C followed by washing 3 times with lysis buffer. Bound resin was resuspended in 60 μl of 2× NuPAGE lithium dodecyl sulfate protein sample buffer (Invitrogen) followed by boiling for 10 min and electrophoresis through NuPAGE 4–12% Bis-Tris gels (Invitrogen). Gels were either silver-stained or used for transfer to polyvinylidene difluoride membranes for Western blotting. Blots were incubated with polyclonal anti-LAR antibody raised against a synthetic peptide corresponding to the LAR membrane proximal domain (RAALEYLGSFDHYAT) or with polyclonal anti-LAR antibody raised against a synthetic peptide corresponding to the LAR C terminus (RGFYNRPISPDLSYQC). Both antibodies would be expected to identify the LAR ~85-kDa intracellular subunit. After LAR antibody, blots were re-probed with polyclonal goat antibody against PTPσ (C18 sc-10871) obtained from Santa Cruz Biotechnology. After incubation with horseradish peroxidase-linked secondary antibody, signal was detected using the ECL chemiluminescence system (Amersham Biosciences).

Co-immunoprecipitation—PC12 cells (1.0×10^6 cells/well) were seeded in a volume of 2 ml of culture medium containing 10% HS and 5% FBS in 6-well plates precoated with poly-L-lysine and incubated overnight. Cells were then washed 3 times with serum-free DMEM and cultured in 2 ml of DMEM containing 0.5% FBS overnight followed by exposure to serum-free DMEM alone or DMEM containing NGF (0.18 nM) or NGF plus peptide (peptide 4 μM) followed by harvesting at 10 min. Aliquots (700–800 μl; 500 μg of protein) of PC12 cell lysates were prepared as described above. Immunoprecipitations were performed by adding preimmune serum (5 μg), polyclonal anti-TrkA antibody (Cell Signaling, Beverly, MA; 1:250 dilution), or polyclonal anti-LAR antibody directed against the LAR C terminus (5 μg) and incubating overnight at 4 °C. Immune complexes were captured by adding 100 μl of protein A-agarose (Pierce) followed by incubation with end-over-end rotation overnight at 4 °C followed by washing 5 times in lysis buffer. Protein was eluted by boiling for 10 min in 100 μl of 2× NuPAGE lithium dodecyl sulfate sample buffer. Aliquots were submitted to NuPAGE 4–12% Bis-Tris gels and transferred to polyvinylidene difluoride membranes. Western blots were incubated with antibody directed against the LAR C terminus or polyclonal anti-TrkA antibody and then incubated with horseradish peroxidase-linked secondary antibodies. Signal was detected using the ECL chemiluminescence system.

PC12 Cell Proliferation—PC12 cell proliferation was quantitated using protocols described in Tisi *et al.* (19). Cells were seeded at a density of 1.5×10^5 cells/well in a total volume of 2 ml/well of DMEM containing 10% HS and 5% FBS in 6-well plates (Corning, Corning, NY) precoated with poly-L-lysine (10 μg/well). Peptides were added at the time of cell seeding. For each of five assays, single or duplicate wells for each peptide condition were assessed. At the indicated times, cells were harvested by adding 0.5 ml of 0.05% trypsin to each well, incubating at 37 °C for 2 min, and collecting the entire cell content of each well. After trituration, aliquots of well mixed cells were counted using a hemocytometer. Intact, round, phase-bright cells that exclude trypan blue were counted, and two aliquots per well were measured and then averaged.

A second set of PC12 cell proliferation studies was conducted using BrdUrd incorporation as a measure of proliferation (33). Cells were seeded on poly-L-lysine-coated 12CIR-1D cover glass slips in 24-well plates (Fisher) by adding 0.25 ml of cell suspension (20,000 cells/cm^2), 0.25 ml of DMEM containing 10% HS and 5% FBS, and wedge peptide (4 μM) to each well. To label newly synthesized DNA, BrdUrd (10 μM) was added to the culture medium for 5 h before fixing in 4% paraformaldehyde. BrdUrd immunostaining was conducted with mouse anti-BrdUrd antibody (DakoCytomation, Glostrup, Denmark) at 1:200 with fluorescein isothiocyanate donkey anti-mouse (Molecular Probes, Invitrogen) at 1:200 serving as the secondary antibody. Using a fluorescence microscope (Leica DM IRE2), six fields were systematically acquired in each of

three assays for each condition. For each image, the number of BrdUrd-positive cells per area was counted in a blinded fashion.

PC12 Cell Survival and Neurite Outgrowth—PC12 cell survival and neurite outgrowth were quantitated using protocols described in Tisi *et al.* (19). 1.5×10^5 cells/well were seeded in a total volume of 2 ml/well of DMEM containing 10% HS and 5% FBS in 6-well plates precoated with poly-L-lysine and allowed to attach for 2 h. After 2 h cells were washed 3 times with serum-free medium, and medium was replaced with serum-free DMEM supplemented with penicillin (100 units/ml) and streptomycin (100 μg/ml). NGF (Invitrogen) or peptides were added to the same medium at concentrations indicated in figure legends. Cells were cultured for durations of 2 or 7 days. In 7-day cultures, on days 2, 4, and 6, 0.5 ml of medium was removed and replaced with 0.5 ml of fresh medium containing NGF or peptide at the original concentration. Cells were fixed with 4% formaldehyde in phosphate-buffered saline, and cell survival was quantitated under phase contrast microscopy by quantitating in a blinded fashion the number of intact, round, phase-bright cells per area. Prior studies demonstrated that morphological-based assessment of surviving cells provided data equivalent to that provided using Syto-13 and propidium iodide cell death indicators (19). Neurite length quantification was performed in a blinded fashion using NIH Image analysis software.

In separate assays, PC12 cell survival was assessed using the established strategy of combined TUNEL and DAPI staining to quantitate the ratio of apoptotic (TUNEL-positive) over total (DAPI-positive) cells. Cells were seeded on poly-L-lysine-coated 12CIR-1D cover glass in 24-well plates (Fisher) by adding 0.25 ml of cell suspension (30,000 cells/cm^2) and 0.25 ml of DMEM containing 10% HS and 5% FBS. After a 2-h attachment period, cells were washed 3 times with serum-free medium, and medium was replaced with serum-free DMEM supplemented with penicillin (100 units/ml) and streptomycin (100 μg/ml) and containing NGF (5 or 50 ng/ml; 0.18 or 1.8 nM) or peptides (4 μM). During the 7-day culture period, on days 2, 4, and 6, 0.25 ml of medium was removed and replaced with 0.25 ml of fresh medium containing NGF or peptide at the original concentration. After 7 days in culture, cell apoptosis was assessed using the fluorescein-12-dUTP, DeadEnd™ Fluorometric TUNEL system (Promega, Madison, WI) and VECTASHIELD® plus DAPI (Vector Labs Burlingame, CA). Samples were analyzed under a fluorescence microscope (Leica DM IRE2) using a standard fluorescence filter set to view green (TUNEL) fluorescence at 520 nm and blue (DAPI) at 460 nm. For each assay, 6 fields were systematically photographed, and DAPI-positive cells were counted as either TUNEL-positive or TUNEL-negative in a blinded fashion. A total of three independent assays were conducted.

Bonhoeffer Stripe Assay—Neural retinas were dissected from embryonic day 8 (stage 32) chick embryos, flattened on concanavalin-coated nitrocellulose filters, and cut into 350-μm wide explants perpendicular to the optic fissure. Explants were placed retinal ganglion side down on substrate-coated dishes and grown in 10% fetal bovine serum (Atlas, Fort Collins, CO), 2% chick serum (Sigma), 2 mM L-glutamine (Invitrogen), 2 units/ml penicillin, 2 μg/ml streptomycin, and 5 ng/ml amphotericin in RPMI 1640 (Invitrogen). The substrate lane assay used was a modified version of the Bonhoeffer method (34), performed as previously described (35). Briefly, tissue culture dishes were coated with nitrocellulose and dried before applying the silicon lane matrix to the dish surface. A PTPμ-Fc chimera, a fusion between the extracellular domain of PTPμ (amino acids 1–621) and the Fc region of immunoglobulin heavy chain (36), was used as the first substrate. PTPμ-Fc chimera (80 ng total) containing a small amount of Texas Red-conjugated BSA (for visualization of the lanes; Molecular Probes) was injected into the channels of the matrix, incubated, aspirated, then replaced with a fresh aliquot of the same substrate. All remaining binding sites within the lanes were blocked with BSA (fraction V; Sigma) and rinsed with calcium-magnesium-free phosphate buffer. The matrix was removed, and 875 ng (total) of laminin (Biomedical Technologies Inc., Stoughton, MA) was spread across the lane area and incubated for 30 min. The entire dish was blocked with BSA and then rinsed with RPMI. Explants were cultured for 48 h before imaging. Representative images from a minimum of three separate experiments are shown.

Quantitation of stripe assays was performed using a rating scale as previously described (37, 38). Neurites that show no preference for either substrate are rated 0, and neurites that grow exclusively on one substrate are rated 3. A rating of 2 indicates that most of the neurites grow on the laminin lanes with an occasional neurite crossing over PTPμ lanes, whereas a rating of 1 is given when there is a significant amount of neurite crossing but a tendency to fasciculate on laminin. Data from a minimum of three experiments were combined (with a minimum sample size of nine explants per condition) to determine the average degree of avoidance for each condition, then analyzed with Fisher's PLSD (Statview 4.51; Abacus Concepts, Inc., Calabasas, CA) at a 95% confidence level.

TrkA Activation in PC12 LAR Antisense Cells—PC12 cells stably transfected with LAR antisense construct or null vector control construct have been described previously (19). In LAR antisense-expressing cells (clone LAS-1) LAR protein levels are reduced to ~35% of levels present in null-transfected control cells (clone LC-2). To assess the effects of LAR deficiency on TrkA activation, 1.0×10^6 cells per well were seeded in a total volume of 2 ml of culture medium containing 5% FBS and 10% HS in 6-well plates precoated with poly-L-lysine and incubated until cells reached ~80% confluence. Cells were washed 3 times with serum-free DMEM and cultured in 2 ml of DMEM containing 0.5% FBS overnight at 37 °C. Cells were then cultured in serum-free DMEM for 4 h followed by exposure to either serum-free DMEM alone or DMEM containing NGF or peptide for 10- or 30-min durations followed by harvesting in lysis buffer.

Western Blot Analysis—Aliquots of PC12 cell lysates containing 15 μg of protein were mixed with NuPAGE lithium dodecyl sulfate protein sample buffer and boiled for 10 min. Samples were then run on NuPAGE 4–12% Bis-Tris gels. Proteins were electrophoretically transferred from gels to polyvinylidene difluoride membranes (Amersham Biosciences) for 1 h at 30 V. Filters were blocked in blocking buffer consisting of 5% nonfat dry milk (Bio-Rad) in TBST (20 mM Tris-HCl, pH 7.5, 137 mM, 0.2% Tween 20) for 1 h at room temperature. After 1 h of blocking, membranes were incubated overnight at 4 °C with one of the following antibodies (all from Cell Signaling): polyclonal anti-phospho-Trk^{Y490}, monoclonal anti-phospho-ERK$^{T202/Y204}$, or monoclonal anti-phospho-AKT^{S473}. Blots were reprobed with polyclonal antibody recognizing total TrkA protein, total ERK1/2 protein, or total AKT protein. Polyclonal goat antibody against PTPσ (C19 sc-10871) was obtained from Santa Cruz Biotechnology. One Western blot was performed in each assay for each cell extract derived from each culture condition. In studies of TrkA activation described in Fig. 7*D*, duplicate Western blots were performed in two of the five assays conducted, and their resulting values were averaged.

RESULTS

Wedge Domain Peptides—The crystal structure of the LAR D1 and D2 catalytic domains and the location of the D1 wedge domain are illustrated in Fig. 1, *A* and *B*. Peptides containing a 24-residue segment corresponding to the LAR wedge HLH domain were synthesized. Inclu-

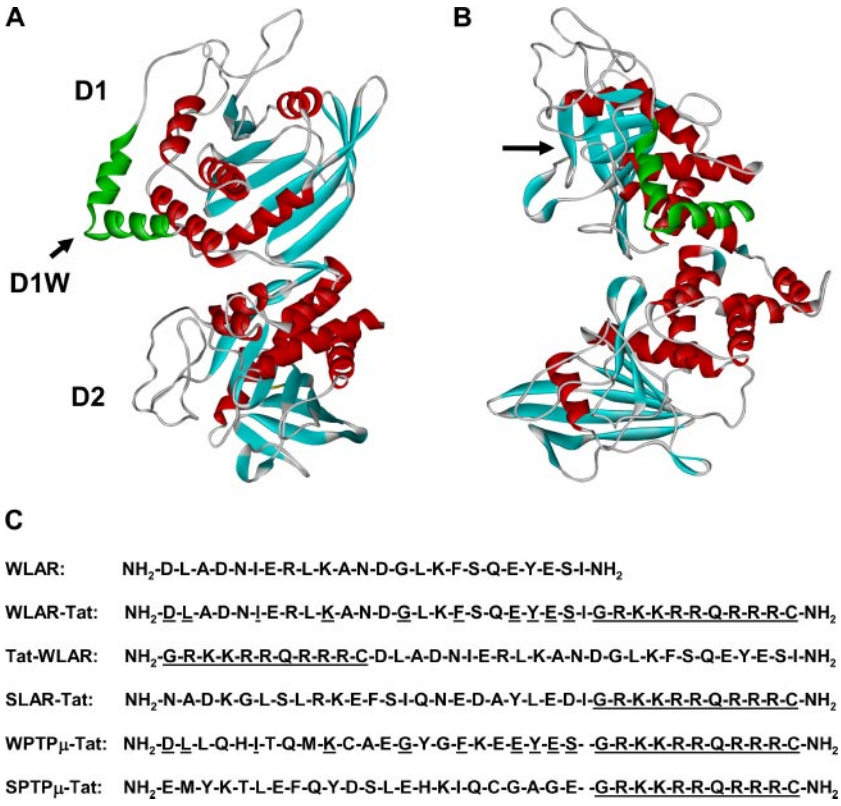

FIGURE 1. **PTP wedge domain peptides.** *A*, tandem catalytic domains (D1 and D2) in the LAR intracellular subunit (modeled after the LAR crystal structure (22)). The wedge domain (*D1W*), located at the N terminus of D1, consists of a HLH structure and is shown in *green*. *B*, rotation of the same structure around the vertical axis 90° counterclockwise reveals the D1 catalytic cleft (*arrow*) adjacent to the wedge domain. *C*, LAR and PTPμ wedge domain peptides were synthesized with an amide substituted for the C terminus: *WLAR*, wedge sequence without Tat; *WLAR-Tat*, wedge sequence with the Tat peptide (Tat sequence is *underlined*) linked to the C terminus; *Tat-WLAR*, wedge sequence with the Tat sequence linked to the N terminus; *SLAR-Tat*, scrambled wedge sequence with the Tat peptide linked to the C terminus; *WPTPμ-Tat*, PTPμ wedge sequence with the Tat peptide linked to the C terminus (*underlined* individual residues in the WLAR-Tat and WPTPμ-Tat sequences are shared, consistent with PTPμ and LAR conserved residues); *SPTPμ-Tat*, scrambled wedge sequence with the Tat peptide linked to the C terminus.

sion of an 11-residue Tat-derived protein transduction domain provides a well established method for delivery of peptides into cells (30). As demonstrated in Fig. 1*C*, four peptides containing the following LAR residues were synthesized, (i) residues containing the wedge sequence alone (WLAR), (ii) the wedge sequence with the Tat domain linked to the C terminus (WLAR-Tat), (iii) the wedge sequence with the Tat domain linked to the N terminus (Tat-WLAR), and (iv) the wedge sequence randomly scrambled with the Tat domain linked to the C terminus (SLAR-Tat). LAR and PTPμ are both members of the type II RPTP subfamily (39, 40). To determine whether the novel principle of inhibiting wedge PTP biological activity with a wedge peptide could be applied to another wedge PTP, a PTPμ wedge peptide (WPTPμ-Tat) corresponding to the analogous LAR wedge sequence along with its scrambled control (SPTPμ-Tat) were synthesized (Fig. 1*C*). All peptides were synthesized with amide groups at the C terminus.

LAR and PTPμ Wedge Peptides Demonstrate Sequence-specific, Homophilic Binding—Fluorescent beads coated with scrambled LAR (SLAR-Tat) or scrambled PTPμ (SPTPμ-Tat) wedge peptide and incubated together in the same mixture failed to demonstrate either homophilic or heterophilic binding (Fig. 2*A*). Uncoated beads and beads coated with BSA also failed to show homophilic binding (not shown). In contrast, beads coated with WLAR-Tat or WPTPμ-Tat and mixed together demonstrated homophilic binding but showed no heterophilic binding (Fig. 2*B*). In additional bead binding assays (data not shown), all three forms of LAR wedge peptides tested, WLAR, WLAR-Tat, and Tat-WLAR, exhibited homophilic binding, demonstrating that binding is not dependent on the presence of the Tat sequence or its location. These studies demonstrated the occurrence of sequence-specific, homophilic interaction between LAR HLH wedge domain peptides and between PTPμ HLH wedge domain peptides, a property previously established for HLH domains in other types of proteins (23–25).

LAR Wedge Peptide Binds to Full-length LAR—To further confirm homophilic binding and to determine whether the LAR wedge peptide

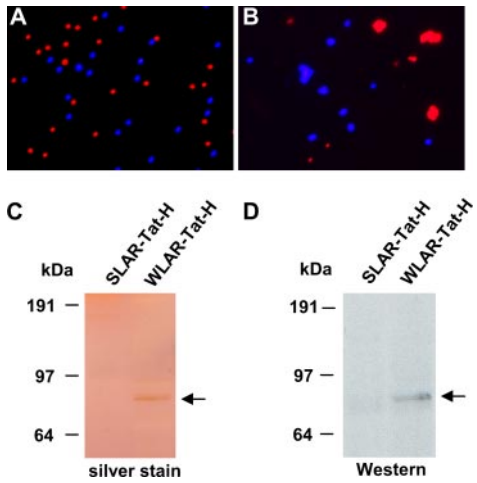

FIGURE 2. **Wedge peptides self aggregate and also pull down LAR.** *A*, beads coated with SLAR-Tat (*red*) or with SPTPμ-Tat (*blue*) were incubated together and show no homophilic or heterophilic binding. *B*, beads coated with WLAR-Tat (*red*) or WPTPμ-Tat (*blue*) were incubated together and demonstrated homogenous *red versus blue* aggregates consistent with homophilic binding and the exclusion of heterophilic binding. *C*, silver-stained gel derived from PAGE analysis of PC12 cell extracts subjected to pull-down assays using SLAR-Tat or WLAR-Tat, each with a polyhistidine tag linked to the C terminus. An ~85-kDa band consistent with LAR is detected in WLAR-Tat but not SLAR-Tat pull-down samples. *D*, Western blot analysis of the same gel performed with an antibody directed against the LAR membrane proximal domain detects ~85-kDa LAR in WLAR-Tat pull-down samples but not in SLAR-Tat samples.

would bind to full-length LAR, WLAR-Tat and SLAR-Tat were synthesized to include a polyhistidine tag linked to the C terminus (WLAR-Tat-H and SLAR-Tat-H). Pull-down assays in which these peptides were incubated in PC12 cell extracts demonstrated that WLAR-Tat-H, but not SLAR-Tat-H, captured the expected ~85-kDa intracellular subunit of the LAR protein (Fig. 2, *C* and *D*). The ability of WLAR-Tat-H to capture LAR provided further evidence that LAR wedge peptide undergoes homophilic interaction and suggested it is capable of binding to the

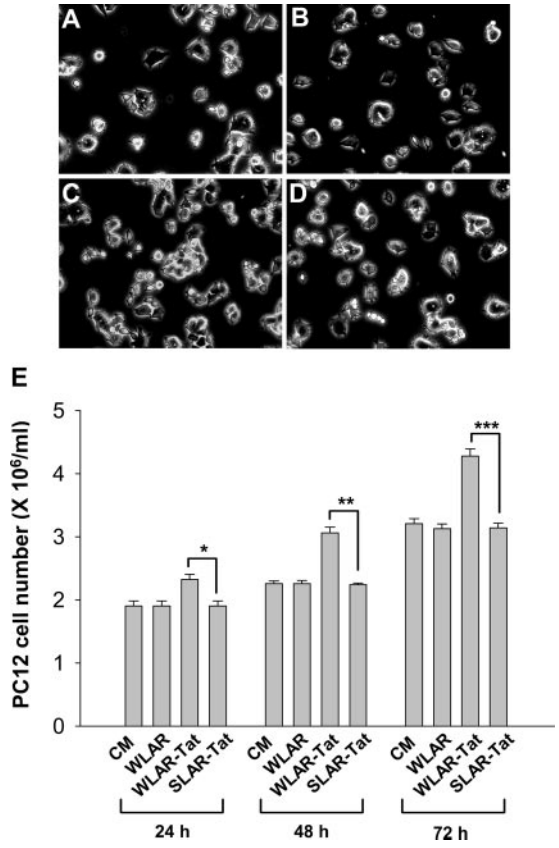

FIGURE 3. **LAR wedge peptide promotes PC12 cell proliferation.** PC12 cells were grown in high serum CM containing no peptide (*A*), WLAR (*B*), WLAR-Tat (*C*), or SLAR-Tat (*D*) and fixed at 72 h. In all conditions, cells were plated in the presence of peptide at 4 μM. In the *panel below* (*E*), PC12 cell number per well at the indicated times is shown. Mean ± S.E., $n = 5$ assays for each condition. *, $p < 0.05$; **, $p < 0.01$; ***, $p < 0.001$ (Student's *t* test).

LAR wedge domain in the context of the full-length LAR intracellular subunit protein. The presence of PTPδ and PTPσ protein in PC12 cells (a rat-derived clone) is not well established. The availability of antibody capable of detecting rat PTPσ allowed Western blot assessment of PC12 cell extract and probing of WLAR-Tat-H pull-down samples. PTPσ antibody failed to detect PTP signal while successfully detecting PTPσ in brain extract control blots (data not shown). Further studies will be required to determine whether LAR wedge peptide binds to PTPδ, PTPσ, and other wedge PTPs.

LAR Wedge Peptides Promote a PC12 Cell Phenotype Resembling That Induced by Antisense-mediated LAR Down-regulation—PC12 cells stably transfected with LAR antisense constructs demonstrate a 65% reduction in LAR protein levels and exhibit a phenotype with the following three features: (i) increased proliferation in serum-containing medium; (ii) decreased cell death and increased neurite outgrowth in serum-free medium; (iii) enhanced neurite outgrowth response to NGF (19). In serum-containing PC12 cell cultures, the addition of WLAR-Tat, but not SLAR-Tat or WLAR, led to a small but statistically significant increase in proliferation as determined by counts of surviving cells at 24, 48, and 72 h (Fig. 3). The lack of effect of WLAR suggested that activity is dependent on Tat-mediated access to its intracellular target. In a separate series of confirmatory studies using BrdUrd labeling as an additional measure of proliferation, WLAR-Tat caused a 17% increase in the proportion of BrdUrd-positive cells at 72 h compared with no effect found with SLAR-Tat ($p < 0.01$, Student's *t* test, $n = 18$ fields, 6 fields from each of 3 independent assays).

In serum-free cultures, the addition of NGF or WLAR-Tat led to significantly increased survival and neurite outgrowth as determined by counts of morphologically intact cells (Fig. 4, *A–C*). The Trk inhibitor K252a blocked the survival- and neurite-promoting effects of both NGF and WLAR-Tat. SLAR-Tat, WLAR, WPTPμ-Tat, and SPTPμ-Tat had no effect on survival or neurite outgrowth. Promotion of cell survival by WLAR-Tat was confirmed in a separate series of studies using TUNEL/DAPI staining to detect cell death (Fig. 4*D*). Dose-response studies measuring NGF-dependent promotion of survival in serum-free medium demonstrated that WLAR-Tat, but not SLAR-Tat, enhanced NGF effects at suboptimal NGF doses (Fig. 5). Similarly, dose-response studies measuring NGF-dependent promotion of neurite outgrowth in serum-free medium showed that WLAR-Tat, but not SLAR-Tat, enhanced NGF effects at suboptimal NGF doses (Fig. 5). At an NGF concentration of 0.08 nM, WLAR-Tat induced survival and neurite outgrowth equivalent to that seen at an NGF concentration ~3-fold higher. Thus, whereas the effects of WLAR-Tat on cell proliferation and on augmenting NGF function were modest, this peptide induced a phenotype concordant with all three of the previously established features of the phenotype previously shown to be induced by LAR down-regulation. In addition, WLAR-Tat augmented NGF neurotrophic activity at suboptimal doses but not at maximum doses, and its activity was blocked by K252a, two lines of evidence suggesting that WLAR-Tat augments NGF signaling.

Peptides were tested on proliferation, survival, and neurite outgrowth at varying concentrations, although the mechanism of Tat-mediated intracellular accumulation would not be expected to necessarily yield typical ligand-receptor dose-response curves. At concentrations of 1 μM, peptides had little or no effect on PC12 cells, and at concentrations $\geq$8–10 μM, PC12 cells demonstrated evidence of toxicity.

PTPμ Wedge Peptide Blocks Retinal Neurite Outgrowth on a PTPμ-coated Substrate—To determine whether the principle of inhibiting PTP function with the application of a wedge peptide could be applied to another PTP, we tested the ability of PTPμ wedge peptide to inhibit a well characterized PTPμ function. One of the best characterized and quantifiable biological functions of PTPμ is its ability to promote neurite outgrowth of chick nasal retinal ganglion cells (35, 40–42). The extracellular domain of PTPμ mediates homophilic cell-cell aggregation (43, 44) and promotes neurite outgrowth of retinal neurons (40, 42). When nasal retinal explants are grown on alternating lanes of PTPμ and laminin, neurites are able to grow and freely cross both the laminin and PTPμ substrate lanes (34). Down-regulation of PTPμ via the expression of PTPμ antisense leads to reduced neurite outgrowth on PTPμ substrate, demonstrating a requirement for neuronal PTPμ function (40). In the same retinal explant assay, application of WPTPμ-Tat wedge peptide markedly inhibited neurite growth and crossing on PTPμ substrate but not laminin substrate, whereas SPTPμ-Tat peptide had no effect on neurite outgrowth on either PTPμ or laminin substrate (Fig. 6, *A* and *B*). These findings confirmed that the ability of PTP wedge peptides to inhibit PTP function could be demonstrated in at least two members of the PTP wedge family, LAR and PTPμ. Consistent with its inability to bind to the PTPμ wedge motif, WLAR-Tat had no effect on retinal neurite outgrowth on a PTPμ substrate (Fig. 6*C*).

To quantify the extent of neurite crossing in the stripe assays, the average degree of avoidance was determined for each condition (see "Experimental Procedures" for explanation). After WPTPμ-Tat wedge peptide addition, the average degree of neurite avoidance changes from 0.75 (little avoidance) for control experiments to 3 (high avoidance, $p < 0.0001$), indicating that the PTPμ wedge inhibitor peptide blocks neurite outgrowth on a PTPμ substrate. Neither the SPTPμ-Tat peptide

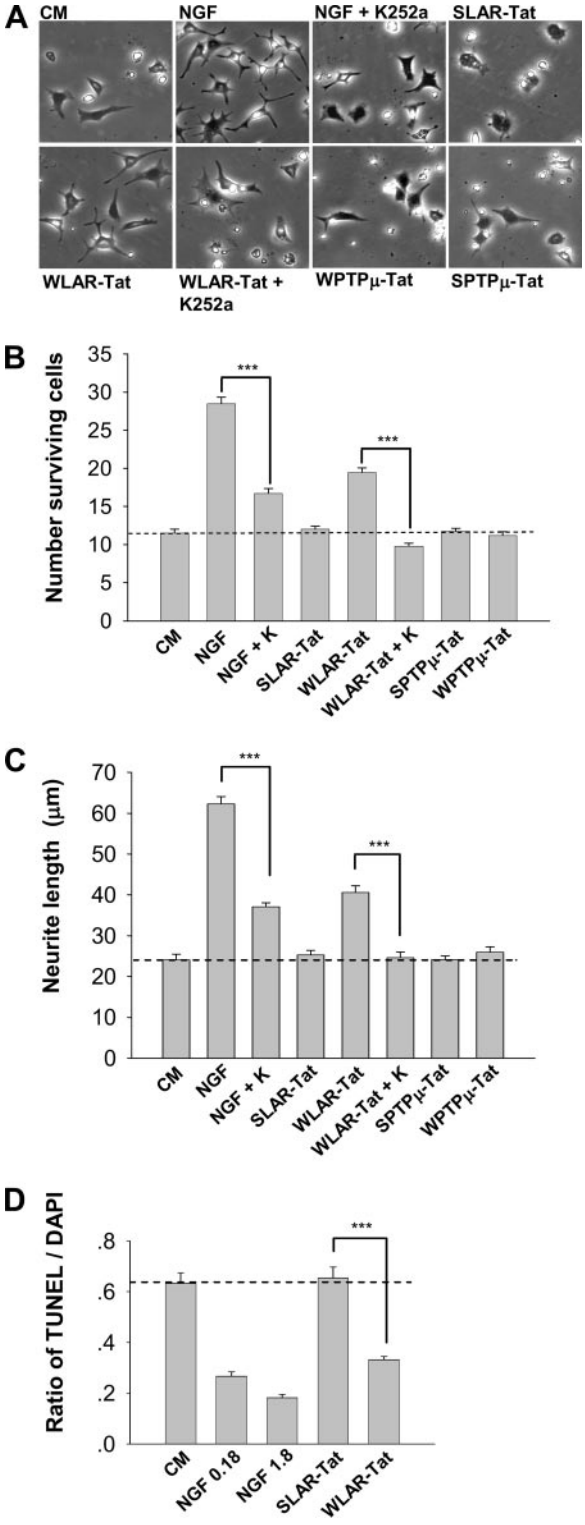

FIGURE 4. **LAR wedge peptide promotes PC12 cell survival and neurite outgrowth.** *A*, PC12 cells were grown in serum-free CM containing NGF, NGF + K252a, SLAR-Tat, WLAR-Tat, WLAR-Tat + K252a (*K*, 200 nM), WPTPμ-Tat, or SPTPμ-Tat. In all conditions, NGF was present at 0.18 nM and K252a at 200 nM, and cells were plated in the presence of peptide at 4 μM. Cell survival was assessed after 7 days. *B* and *C*, quantitation of the number of cells surviving per area and mean neurite length is shown. Mean ± S.E. For survival data, $n = 75$ fields counted (25 fields in each of 3 assays). For neurite length data, $n = 78–298$ neurites were measured per condition; for each cell, the longest neurite present was measured. NGF and WLAR-Tat promoted significantly greater survival and neurite outgrowth than that found at base line (culture medium and indicated by *horizontal dashed line*), $p < 0.001$, Student's *t* test. Survival and neurite outgrowth promoted by NGF were significantly decreased in the presence of K252a (***, $p < 0.001$), and survival and neurite outgrowth promoted by WLAR-Tat were entirely blocked by K252a (***, $p < 0.001$). PTPμ peptides failed to promote survival or neurite outgrowth. *D*, TUNEL/DAPI staining was used to detect cell death and confirmed that WLAR-Tat, but not SLAR-Tat, inhibits cell death as indicated by the significantly decreased proportion of TUNEL-positive cells ($n = 18$ fields counted, 6 fields from each of 3 assays; ***, $p < 0.001$, Student's *t* test). Peptides were present at 4 μM, and NGF was at the indicated concentrations.

nor the WLAR-Tat peptide had any quantifiable effect on the average degree of avoidance on a PTPμ substrate. The findings that PTPμ wedge peptide blocked neurite outgrowth on PTPμ whereas the LAR peptide had no effect provide a third line of evidence that LAR and PTPμ wedge peptides are specific to their corresponding receptor PTP.

LAR Associates with TrkA and LAR Deficiency Promotes TrkA Activation—The findings that the Trk inhibitor K252a blocked the survival and neurite promoting effect of WLAR-Tat and that WLAR-Tat augmented suboptimal but not maximal concentrations of NGF raised the possibility that LAR might associate directly or indirectly with TrkA and that inhibition of LAR may up-regulate TrkA signaling. The identity of RPTPs that associate with Trk receptors remain to be established. To determine whether LAR associates with TrkA, reciprocal co-immunoprecipitation studies were performed. Immunoprecipitation with anti-TrkA antibody captured LAR (Fig. 7*A*) and immunoprecipitation with anti-LAR antibody captured TrkA (Fig. 7*B*), indicating that LAR is associated directly or indirectly with TrkA. The addition of NGF did not appear to have a large effect on the ability of LAR immunoprecipitation to capture TrkA (Fig. 7*B*). Interestingly, the addition of WLAR-Tat, but not SLAR-Tat, blocked the ability of LAR immunoprecipitation to capture TrkA (Fig. 7*B*). These findings supported the hypothesis that LAR wedge peptide might interfere with the ability of LAR to interact with TrkA or with proteins mediating LAR-TrkA interaction.

To determine whether down-regulation of LAR leads to augmented TrkA signaling, activation of TrkA was monitored by measuring the phosphorylation of the Tyr-490 site; transphosphorylation of Tyr-490 is a well characterized proximal step in TrkA activation and is required for downstream signaling (5). In PC12 cells, NGF induces TrkA activation with peak activation occurring at 5–10 min and is down-regulated by 30 min (45). At the 10-min time point, NGF induced an ~80% increase in TrkA Tyr-490 phosphorylation in null-transfected control cells and an ~140% increase in LAR antisense PC12 cells (Fig. 7, *C* and *D*). At the 30-min time point, TrkA Tyr-490 phosphorylation was similar between the two cell types, indicating that LAR down-regulation increased the early peak phase of TrkA activation but did not lead to a sustained augmentation of TrkA activation. The finding of enhanced NGF-induced TrkA activation in LAR-antisense cells along with evidence that LAR wedge peptide interferes with LAR function predicted that a LAR wedge peptide might similarly activate TrkA and/or augment early phase NGF-induced TrkA activation. The addition of WLAR-Tat peptide led to TrkA activation to a level significantly above base line and ~50% of that seen with NGF-induced activation at the 10 min time point, whereas SLAR-Tat had no effect (Fig. 7, *E* and *F*). The addition of WLAR-Tat, but not SLAR-Tat, to a submaximal concentration of NGF (0.18 nM) led to an ~2-fold augmentation of NGF-induced TrkA activation at the 10-min time point (Fig. 7, *G* and *H*). Taken together, these findings indicate that down-regulation of LAR expression augments TrkA activation and that the LAR wedge peptide, possibly by interfering with LAR function, also promotes and/or augments TrkA activation. The ability of the LAR wedge peptide to trigger TrkA activation in the absence of added NGF could be due to augmentation of the effects of trace levels of endogenous NGF potentially present in cultures or, alternatively, might result from potentiation of otherwise undetectable basal levels of non-ligand-dependent TrkA activation.

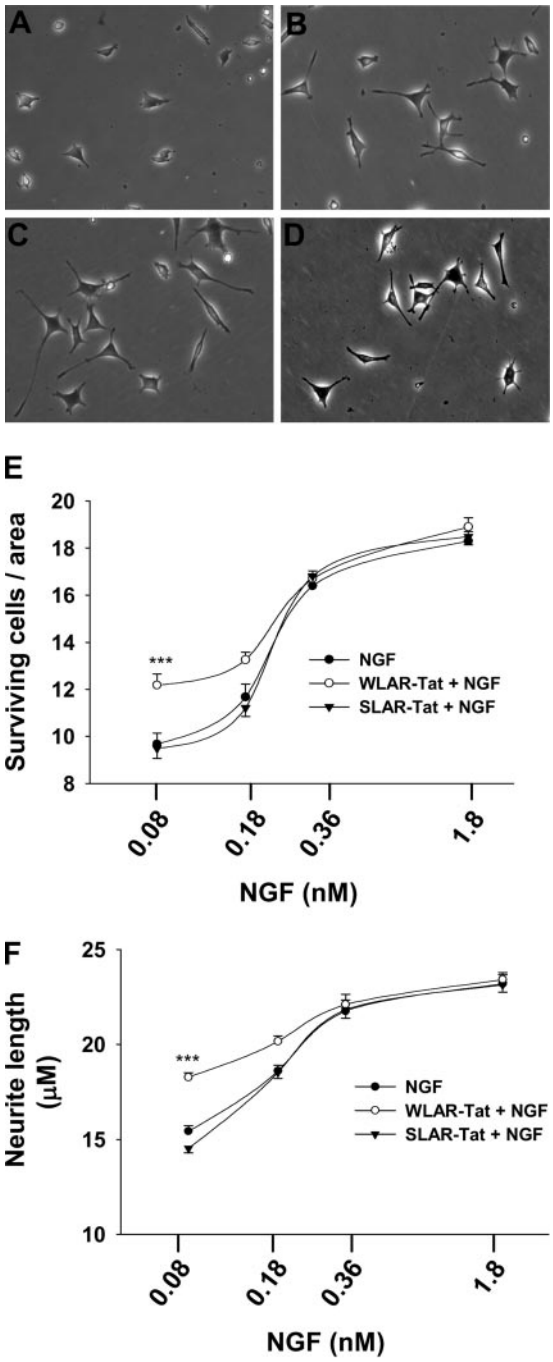

FIGURE 5. **LAR wedge peptide augments NGF promotion of survival and neurite outgrowth.** PC12 cells were incubated under the following serum-free conditions and fixed after 48 h. *A*, CM alone; *B*, NGF (0.08 nM); *C*, NGF (0.08 nM) + WLAR-Tat (4 μM); *D*, NGF (0.08 nM) + SLAR-Tat (4 μM). In the presence of NGF combined with WLAR-Tat (*C*), greater numbers of surviving cells and longer neurites were observed. Quantitative morphological analysis of the same cultures assessed NGF promotion of PC12 cell survival (*E*) in the absence of peptide and in the presence of SLAR-Tat or WLAR-Tat present at fixed concentrations of 4 μM. The number of microscopic fields counted for each NGF dose and condition ranged from 48 to 96, derived from 4 independent assays. NGF promotion of PC12 cell neurite outgrowth (*F*) was assessed in the absence of peptide and in the presence of SLAR-Tat or WLAR-Tat at fixed concentrations of 4 μM. The number of neurites measured for each NGF dose and condition ranged from 840 to 1760, derived from 4 independent assays. At the NGF dose of 0.08 nM, WLAR-Tat augmented NGF-induced survival and neurite outgrowth; ***, $p < 0.001$, Student's *t* test.

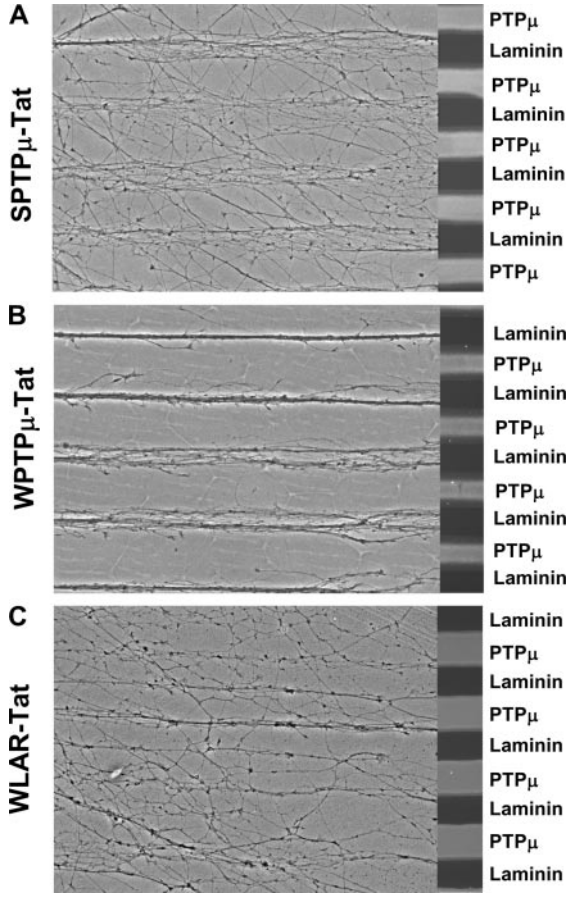

FIGURE 6. **PTPμ but not LAR wedge peptide blocks neurite outgrowth of nasal retinal ganglion cells on a PTPμ substrate.** Embryonic day 8 chick nasal retinal explants were grown on alternating stripes of PTPμ-Fc chimera and laminin and incubated with either SPTPμ-Tat (*A*), WPTPμ-Tat (*B*), or WLAR-Tat peptides (*C*), each added at a final concentration of 4 μM. Phase contrast images (*left side* of *panels*) display the extent of neurite outgrowth and crossing between the substrates, whereas the fluorescent images (*right side* of *panels*) illustrate the alternating substrate lanes of PTPμ-Fc/Texas Red BSA and laminin. In the presence of SPTPμ-Tat (*A*), neurites readily cross between the substrate lanes, a pattern identical to that occurring in the absence of peptide (not shown), indicating that both substrates are permissive for neurite outgrowth. In contrast, incubation with WPTPμ-Tat (*B*) markedly reduces neurite crossing of the PTPμ-Fc substrate. The LAR wedge peptide, WLAR-Tat (*C*) has no effect on neurite crossing of the PTPμ-Fc substrate. Thus, the ability to block PTPμ-dependent neurite outgrowth is specific to PTPμ wedge peptide.

LAR Wedge Peptide Promotes TrkA Downstream Signaling—The finding that WLAR-Tat activates TrkA predicted that WLAR-Tat would also activate TrkA downstream signaling. Both ERK activation and AKT activation are downstream consequences of TrkA signaling and are readily measured using phospho-specific antibodies to the activated form of the enzyme. Extracts derived from the 10-min time point of the same cultures used for assessment of TrkA activation (Fig. 7) were used to measure activation of ERK and AKT. WLAR-Tat led to ERK activation to a level of ~60% that induced by NGF, whereas SLAR-Tat had no effect (Fig. 8, *A* and *B*). The addition of WLAR-Tat, but not SLAR-Tat, to a submaximal concentration of NGF (0.18 nM) led to a significant augmentation of NGF-induced ERK activation by ~1.6-fold (Fig. 8, *C* and *D*). In studies of AKT activation, WLAR-Tat promoted activation to a level ~75% that stimulated by NGF, whereas SLAR-Tat had no effect (Fig. 8, *E* and *F*). The addition of WLAR-Tat to a submaximal concentration of NGF (0.18 nM) led to a significant 1.4-fold augmentation of NGF-induced AKT activation, whereas SLAR-Tat had no effect (Fig. 8, *G* and *H*). These findings demonstrated that the LAR wedge peptide augments (and also potentially promotes) activation of two well characterized signaling components downstream of TrkA known to play roles in survival and differentiation of PC12 cells.

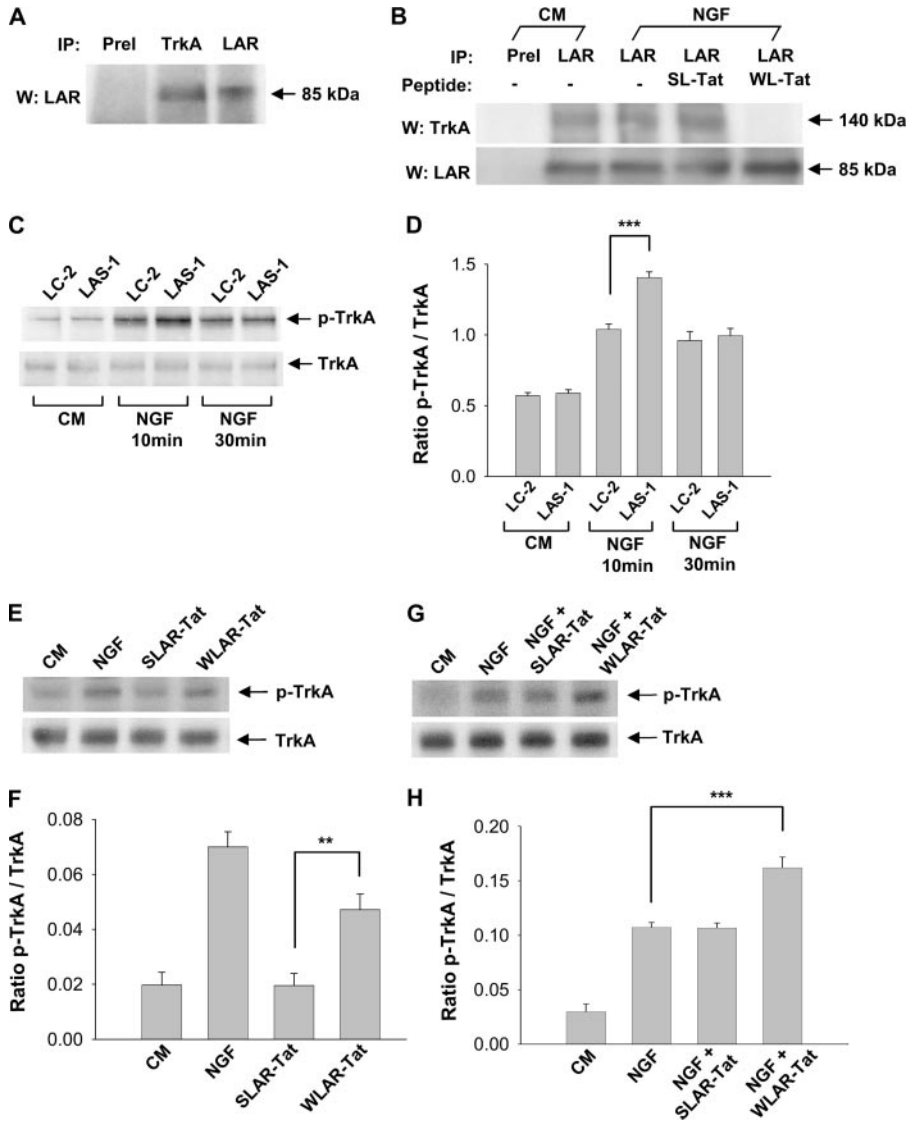

FIGURE 7. **LAR associates with TrkA and regulates its activation.** *A*, PC12 cell extract coimmunoprecipitates (*IP*) formed using preimmune serum (*Prel*), anti-TrkA antibody, or anti-LAR antibody (directed against the LAR C terminus) were assessed by Western blot (*W*) using LAR C terminus antibody. LAR is captured in anti-TrkA and anti-LAR antibody immunoprecipitates. *B*, immunoprecipitates formed using preimmune antibody or anti-LAR antibody (directed against the LAR C terminus) were assessed by Western blot using anti-TrkA antibody followed by re-probing with anti-LAR antibody. TrkA and LAR are captured in anti-LAR antibody immunoprecipitates. Exposure of PC12 cells for 10 min to either CM or NGF (0.18 nM) did not affect TrkA/LAR association. The addition of WLAR-Tat (*WL-Tat*), but not SLAR-Tat (*SL-Tat*), inhibited TrkA association with LAR. *C*, Western blot analysis for phospho-TrkA Tyr-490 (*upper panel*) and total TrkA protein (*lower panel*) in extracts derived from control null-transfected PC12 cells (*LC-2*) and in LAR antisense-transfected LAR-deficient PC12 cells (*LAS-1*) in the absence of NGF (CM) and after NGF (1.80 nM) treatment for the indicated durations. *D*, quantitation of Western blot signal demonstrates augmented NGF-induced activation of TrkA in LAR-deficient cells at the 10 min time point (***, $p < 0.001$; $n = 5$ assays; Student's *t* test). *E*, Western blot analysis for phospho-TrkA (*upper panel*) and total TrkA protein (*lower panel*) in PC12 cells treated with CM, NGF (0.18 nM), SLAR-Tat (4 μM), or WLAR-Tat (4 μM). *F*, quantitation of Western blot signal demonstrates the expected TrkA activation by NGF and also significant TrkA activation by WLAR-Tat compared with SLAR-Tat control (**, $p < 0.001$; $n = 6$ assays). *G*, Western blot analysis for phospho-TrkA (*upper panel*) and total TrkA (*lower panel*) in PC12 cells treated with CM, NGF (0.18 nM), NGF (0.18 nM) + SLAR-Tat (4 μM), or NGF (0.18 nM) + WLAR-Tat (4 μM). *H*, quantitation of Western blot signal demonstrates the expected TrkA activation by NGF and a significant augmentation of TrkA activation by WLAR-Tat compared with SLAR-Tat control (***, $p < 0.001$; $n = 6$ assays).

DISCUSSION

The present study demonstrates that HLH wedge domain peptides corresponding to two members of the RPTP type II family undergo sequence-specific homophilic binding. LAR wedge peptide, but not PTPμ wedge peptide, induces a LAR-deficient phenotype in PC12 cells, whereas PTPμ wedge peptide, but not LAR wedge peptide, promotes a PTPμ-deficient phenotype in retinal ganglion cells. In addition, this work describes the first identification of a RPTP associating with a Trk receptor and reveals that antisense-mediated down-regulation of LAR or use of LAR wedge peptide in PC12 cells leads to increased TrkA activation and increased TrkA downstream signaling. These findings point to two novel potential therapeutic strategies. First, targeting of PTP HLH wedge domains might provide an approach for development of small molecules inhibiting wedge-containing RPTP function. Second, the present work is the first to demonstrate that targeting of a RPTP associated with a Trk receptor can lead to augmentation of receptor activation, downstream signaling, and neurotrophic effects.

The function of the LAR and PTPμ wedge domains remains unknown. In the case of RPTPα and CD45, crystal structure analyses suggest an intermolecular interaction in which receptor dimerization leads to the wedge domain of each monomer, interacting with the D1 catalytic cleft of the adjacent monomer, thereby interfering with catalytic activity (46). In the case of LAR, there is no evidence that an analogous intermolecular interaction inhibits catalytic activity. Crystal structure studies of LAR indicate that steric hindrance by D2 makes an analogous intermolecular interaction unlikely but leaves open the possibility of an intramolecular association between D1 and D2 (22). Similar studies for PTPμ also suggest that an intermolecular inhibitory mechanism is unlikely (47). Yeast two-hybrid screening demonstrated that PTPδ D2 binds in a wedge-dependent manner to PTPσ-D1 and inhibits its catalytic activity (48, 49). Co-immunoprecipitation studies suggest that LAR D1 containing the wedge segment interacts with LAR D2, although the role of the wedge domain in this interaction and whether D2 binding inhibits D1 catalytic activity are not known (50). Intramolecular interactions between the membrane-distal tyrosine phosphatase domain and the juxtamembrane domain of PTPμ have been demonstrated to occur, which reduce PTPμ catalytic activity (51). Yeast interaction trap assays have identified proteins that bind to LAR D2 including Trio (52) and the liprin LAR-interacting proteins (53); however, proteins binding to the LAR wedge domain remain to be identified.

The lack of knowledge regarding LAR intra- and intermolecular interactions as well as the identity of LAR enzymatic substrates within PC12 cells and neurons limits the extent to which the molecular mech-

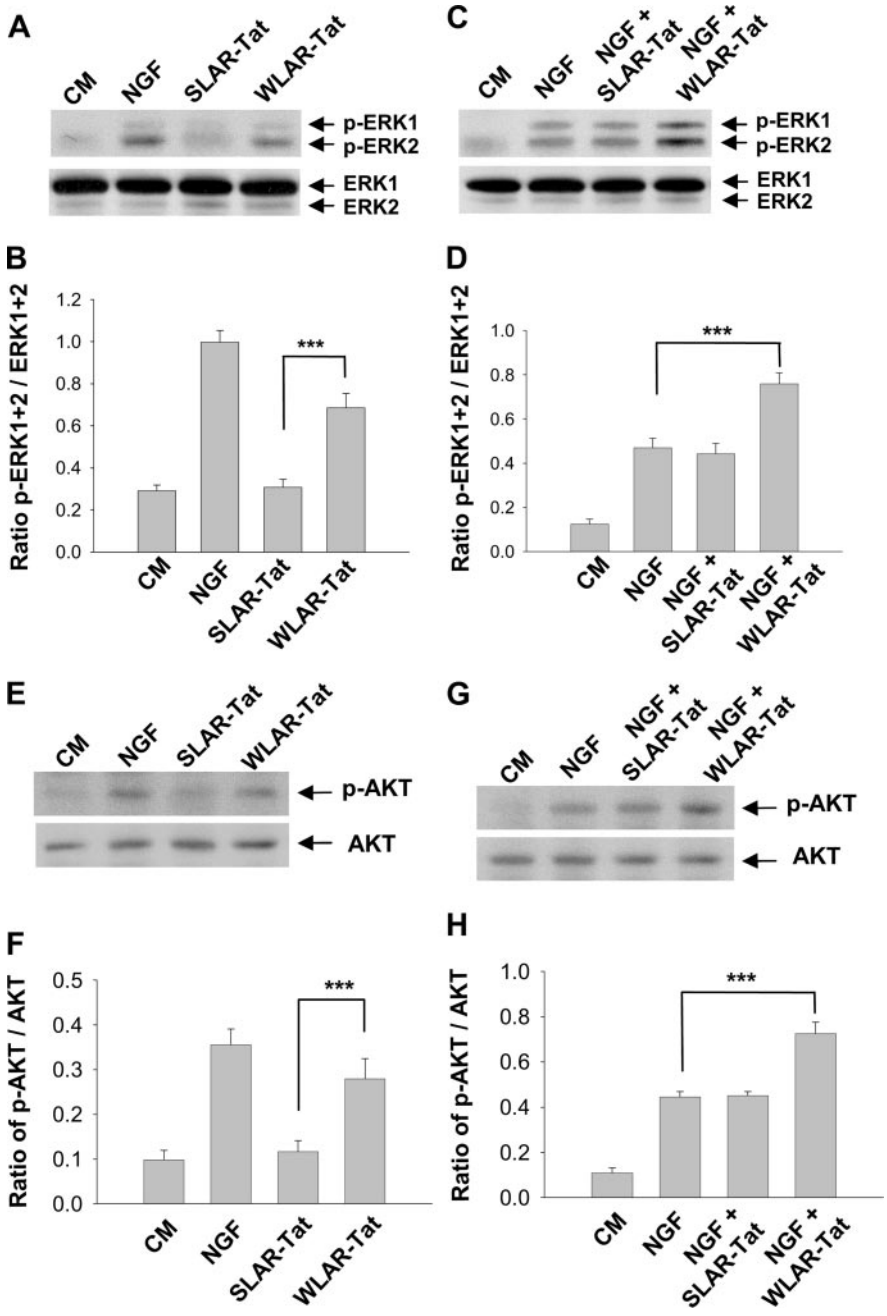

FIGURE 8. **LAR wedge peptide activates ERK and AKT.** The same PC12 extracts assessed in Fig. 7*E*-H were analyzed for activation of ERK and AKT. *A*, Western blot analysis for phospho (*p*)-ERK1 and ERK2 (*upper panel*) and total ERK1 and ERK2 (*lower panel*) in PC12 cells treated with CM, NGF (0.18 nM), SLAR-Tat (4 μM), or WLAR-Tat (4 μM). *B*, quantitative analysis of Western blot signal demonstrates the expected NGF-induced ERK (values of ERK1 and ERK2 are added). WLAR-Tat induced significant ERK activation (***, $p < 0.001$; $n = 6$ *assays*, Student's *t* test), whereas SLAR-Tat had no effect. *C*, Western blot analysis for phospho-ERK1 and ERK2 (*upper panel*) and total ERK1 and ERK2 protein (*lower panel*) in PC12 cells treated with CM, NGF (0.18 nM), NGF (0.18 nM) + SLAR-Tat (4 μM), or NGF (0.18 nM) + WLAR-Tat (4 μM). *D*, quantitative assessment of Western blot signal demonstrates a significant augmentation of NGF-induced ERK activation (***, $p < 0.001$; $n = 6$ assays) by WLAR-Tat, whereas SLAR-Tat had no effect. *E*, Western blot analysis for phospho-AKT (*upper panel*) and total AKT protein (*lower panel*) of the same PC12 cell extracts assessed for ERK activation. *F*, quantitative analysis of Western blot signal demonstrates the expected NGF induction of AKT. WLAR-Tat induced a significant activation of AKT (***, $p < 0.001$; $n = 6$ assays), whereas SLAR-Tat had no effect. *G*, Western blot analysis for phospho-AKT (*upper panel*) and total AKT protein (*lower panel*) of the same PC12 cell extracts assessed for ERK activation. *H*, quantitative assessment of Western blot signal demonstrates a significant augmentation of NGF-induced AKT activation (***, $p < 0.001$; $n = 6$ assays) by WLAR-Tat, whereas SLAR-Tat had no effect.

anisms of action for the wedge peptide can currently be established. There are at least five potential mechanisms by which wedge peptide might interfere with LAR function. First, binding of wedge peptide to the LAR wedge domain might interfere with the ability of LAR to interact with heretofore unidentified adaptors or other functionally important proteins. This possibility is supported by the present finding that LAR wedge peptide blocks LAR-TrkA association either by blocking direct interaction with TrkA or with proteins mediating such interaction. Second, binding of wedge peptide to the LAR wedge domain might interfere with functionally important, activity-promoting, intramolecular interactions between the wedge domain and D2 or other LAR domains. Third, binding of wedge peptide to the wedge domain of LAR might interfere with access of one or more substrates to the D1 enzymatic site. Fourth, wedge peptide might bind to and thereby inhibit adaptors or other proteins normally bound by endogenous LAR via its wedge domain. A fifth and less likely mechanism by which the LAR wedge peptide might inhibit LAR function would involve binding at a non-wedge site located within the LAR catalytic cleft to directly interfere with enzymatic function. This alternative would imply that the wedge peptide is capable of both isologous homophilic binding to the wedge domain and also of binding in a heterologous manner to the LAR catalytic site. The demonstration that a wedge peptide induces a phenotype similar to that achieved by antisense-mediated down-regulation of LAR and enhances signaling of a LAR-associated PTK receptor will provide a rationale for the extensive series of studies that will be required to establish the occurrence of one or more these potential mechanisms. Similar molecular mechanisms could be proposed for the ability of the PTPμ wedge peptide to block known PTPμ-dependent functions. The present work will encourage determination of whether wedge peptides corresponding to other wedge-containing RPTPs will inhibit function.

The rationale for testing the hypothesis that LAR wedge peptides

might down-regulate LAR function stems from the precedent that HLH homophilic binding can block protein-protein interactions and lead to loss of function. Members of the Id transcription factor family, containing a HLH domain but lacking a DNA binding domain, bind to intact HLH-containing transcription factors to form inactive complexes incapable of DNA binding and thereby inhibit function (26, 27). In the case of LAR, the existence of intramolecular and intermolecular binding interactions involving the HLH wedge domain remain to be established, but interference with either mode of interaction would have the potential to inhibit LAR function. An important strategic advantage of the empiric approach applied here is that a given domain, such as the LAR wedge segment, can be targeted before elucidation of its functions and intra- and/or intermolecular interactions. Our findings here will stimulate the elucidation of PTP wedge domain function in LAR and other RPTPs.

The findings that LAR wedge peptides do not bind to PTPμ wedge peptides, that WPTPμ-Tat had no effect on LAR-dependent functions in PC12 cells, and that LAR wedge peptide did not inhibit PTPμ function suggest some degree of specificity among wedge peptides and wedge PTPs. However, further studies that include all wedge PTPs and their corresponding wedge peptides and all possible combinations of wedge PTPs and peptides will be necessary to fully evaluate the degree of specificity that can be obtained with this approach.

Before the present studies, no RPTPs were known to associate with Trk receptors and modulate signaling. The SHP-1 non-receptor PTP co-immunoprecipitates with TrkA in PC12 cells and sympathetic neurons and dephosphorylates TrkA (54). Expression of a dominant-negative SHP-1 mutant in PC12 cells led to activation of TrkA and AKT but not ERK and promoted survival but not neurite outgrowth. This pattern was consistent with studies showing that AKT promotes PC12 cell survival, whereas the ERK pathway promotes neurite outgrowth (5, 55). Given these distinct effects of AKT and ERK signaling, it is of particular interest to note that targeting of LAR with the wedge peptide led to activation of Trk along with both AKT and ERK and to promotion of both survival and neurite outgrowth. The present findings of increased Trk phosphorylation in LAR-deficient PC12 cells along with LAR/TrkA association suggest that LAR may directly or indirectly promote the dephosphorylation of Trk tyrosine residues. Augmentation of TrkA, AKT, and ERK activation is likely one important mechanism by which the wedge peptide augments neurotrophic function and a mechanism that is consistent with LAR-TrkA interaction. Additional studies might identify other neurotrophic pathways activated by LAR wedge peptides.

Because LAR has been shown to regulate signaling by a number of PTKs (32), it is possible that wedge-mediated inhibition of LAR function might lead to up-regulation of PTKs in addition to TrkA. The previous finding that down-regulation of LAR leads to increased epidermal growth factor (EGF) signaling (32) and the well established role for EGF in promoting PC12 cell proliferation (56) raise the possibility that the wedge peptide-induced proliferation of PC12 cells found in the present study might be mediated by up-regulated EGF signaling. Interestingly, the degree of increased proliferation induced by the LAR wedge peptide is relatively modest, perhaps consistent with the ability of TrkA activation (also induced by the wedge peptide) to inhibit proliferation and promote differentiation. Moreover, long term exposure of PC12 cells to NGF has been shown to decrease proliferative response to EGF (57). The present studies will encourage efforts to determine whether targeting of the LAR wedge domain in PC12 cells leads to up-regulation of EGF and other PTK receptors.

The possibility that wedge peptides might act via homophilic binding to the LAR and PTPμ wedge domains raises the important prospect that non-peptide small molecules binding to these wedge domains and interfering with their intra- or intermolecular interactions might offer a novel small molecule approach to inhibiting activity of LAR, PTPμ, and other wedge-containing RPTPs. Such compounds might also create a novel small molecule approach for augmentation of Trk and other PTK signaling. The finding that LAR and PTPμ wedge peptides induce homophilic binding of fluorescent beads provides a basis for high throughput screening for such compounds.

REFERENCES

1. Hunter, T. (1996) *Cell* **80,** 225–236
2. Bixby, J. L. (2000) *Neuroreport* **11,** 5–10
3. Tonks, N. K., and Neel, B. G. (2001) *Curr. Opin. Cell Biol.* **13,** 182–195
4. Ostman, A., and Bohmer, F.-D. (2001) *Trends Cell Biol.* **11,** 258–266
5. Kaplan, D. R., and Miller, F. D. (2000) *Curr. Opin. Neurobiol.* **10,** 381–391
6. Huang, E. J., and Reichardt, L. F. (2003) *Annu. Rev. Biochem.* **72,** 609–642
7. Streuli, M., Krueger, N. X., Thai, T., Tang, M., and Saito, H. (1990) *EMBO J.* **9,** 2399–2407
8. Zhang, J. S., and Longo, F. M. (1995) *J. Cell Biol.* **128,** 415–431
9. Yeo, T. T., Yang, T., Massa, S. M., Zhang, J. S., Honkaniemi, J., Butcher, L. L., and Longo, F. M. (1997) *J. Neurosci. Res.* **47,** 348–360
10. Zhang, J. S., Honkaniemi, J., Yang, T., Yeo, T. T., and Longo, F. M. (1998) *Mol. Cell. Neurosci.* **10,** 271–286
11. Stoker, A. W. (2001) *Curr. Opin. Neurobiol.* **11,** 95–102
12. Xie, Y. M., Yeo, T. T., Zhang, C., Yang, T., Tisi, M. T., Massa, S. M., and Longo, F. M. (2001) *J. Neurosci.* **21,** 5130–5138
13. Van der Zee, C. E. E. M., Man, T. Y., Van Lieshout, E. M. M., Van der Heijden, I., Van Bree, M., and Hendriks, W. J. A. J. (2003) *Eur. J. Neurosci.* **17,** 991–1005
14. Johnson, K. G., and Van Vactor, D. (2003) *Physiol. Rev.* **83,** 1–24
15. Yang, T., Bernabeu, R., Xie, Y.-M., Zhang, J. S., Massa, S. M., Rempel, H. C., and Longo, F. M. (2003) *J. Neurosci.* **23,** 3353–3363
16. Longo, F. M., Martignetti, J. A., LeBeau, J. M., Zhang, J. S., Barnes, J. P., and Brosius, J. (1993) *J. Biol. Chem.* **268,** 26503–26511
17. Bilderback, T. R., Gazula, V.-R., Lisanti, M. P., and Dobrowsky, R. T. (1999) *J. Biol. Chem.* **274,** 257–263
18. Caselli, A., Mazzinghi, B., Camici, G., Manao, G., and Ramponi, G. (2002) *Biochem. Biophys. Res. Commun.* **296,** 692–697
19. Tisi, M. A., Xie, Y., Yeo, T. T., and Longo, F. M. (2000) *J. Neurobiol.* **43,** 477–486
20. Zhang, Z.-Y. (2002) *Annu. Rev. Pharmacol. Toxicol.* **42,** 209–234
21. Bilwes, A. M., den Hertog, J., Hunter, T., and Noel, J. P. (1996) *Nature* **382,** 555–559
22. Nam, H.-J., Poy, F., Krueger, N. X., Saito, H., and Frederick, C. A. (1999) *Cell* **97,** 449–457
23. Goldfarb, A. N., Lewandowska, K., and Shoham, M. (1996) *J. Biol. Chem.* **271,** 2683–2688
24. Massari, M. E., and Murre, C. (2000) *Mol. Cell. Biol.* **20,** 429–440
25. Olson, V. A., Wetter, J. A., and Friesen, P. D. (2001) *J. Virol.* **75,** 6042–6051
26. Benezra, R., Davis, R. L., Lockshon, D., Turner, D. L., and Weintraub, H. (1990) *Cell* **61,** 49–59
27. Ruzinova, M. B., and Benezra, R. (2003) *Trends Cell Biol.* **13,** 410–418
28. Nieddu, E., Melchiori, A., Pescarolo, M. P., Bagnasco, L., Biasotti, B., Licheri, B., Malacarne, D., Tortolina, L., Castagnino, N., Pasa, S., Cimoli, G., Avignolo, C., Ponassi, R., Balbi, C., Patrone, E., D'Arrigo, C., Barboro, P., Vasile, F., Orecchia, P., Carnemolla, B., Damonte, G., Millo, E., Palomba, D., Fassina, G., Mazzei, M., and Parodi, S. (2005) *FASEB J.* **19,** 632–634
29. Souroujon, M. C., and Mochly-Rosen, D. (1998) *Nat. Biotechnol.* **16,** 919–924
30. Wadia, J. S., and Dowdy, S. F. (2002) *Curr. Opin. Biotech.* **13,** 52–56
31. Beattie, E. C., Zhou, J., Grimes, M. L., Bunnett, N. W., Howe, C. L., and Mobley, W. C. (1996) *Cold Spring Harbor Symp. Quant. Biol.* **61,** 389–406
32. Kulas, D. T., Goldstein, B. J., and Mooney, R. A. (1996) *J. Biol. Chem.* **271,** 748–754
33. Perry, T., Lahiri, D. K., Chen, D., Zhou, J., Shaw, K. T. Y., Egan, J. M., and Greig, N. H. (2002) *J. Pharmacol. Exp. Ther.* **300,** 958–966
34. Vielmetter, J., Stolze, B., Bonhoeffer, F., and Stuermer, C. A. (1990) *Exp. Brain Res.* **81,** 283–287
35. Burden-Gulley, S. M., Ensslen, S., and Brady-Kalnay, S. M. (2002) *J. Neurosci.* **22,** 3615–3627
36. Rosdahl, J. A., Ensslen, S. E., Niedenthal, J. A., and Brady-Kalnay, S. M. (2003) *J. Neurobiol.* **56,** 199–208
37. Walter, J., Kern-Veits, B., Huf, J., Stolze, B., and Bonhoeffer, F. (1987) *Development* **101,** 685–696
38. Ensslen, S., and Brady-Kalnay, S. M. (2004) *Mol. Cell. Neurosci.* **25,** 558–571
39. Brady-Kalnay, S. M. (2001) in *Cell Adhesion: Frontiers in Molecular Biology* (Beckerle, M., ed) Vol. 39, pp. 217–258, Oxford University Press, Oxford, UK

40. Ensslen-Craig, S. E., and Brady-Kalnay, S. M. (2005) *Mol. Cell. Neurosci.* **28,** 177–188
41. Ensslen-Craig, S. E., and Brady-Kalnay, S. M. (2004) *Dev. Biol.* **275,** 12–22
42. Burden-Gulley, S., and Brady-Kalnay, S. M. (1999) *J. Cell Biol.* **144,** 1323–1336
43. Brady-Kalnay, S. M., Flint, A. J., and Tonks, N. K. (1993) *J. Cell Biol.* **122,** 961–972
44. Brady-Kalnay, S. M., and Tonks, N. K. (1994) *J. Biol. Chem.* **269,** 28472–28477
45. Zhou, J., Valletta, J. S., Grimes, M. L., and Mobley, W. C. (1995) *J. Neurochem.* **65,** 1146–1156
46. Majeti, R., and Weiss, A. (2001) *Chem. Rev.* **101,** 2441–2448
47. Hoffmann, K. M., Tonks, N. K., and Barford, D. (1997) *J. Biol. Chem.* **272,** 27505–27508
48. Wallace, M. J., Fladd, C., Batt, J., and Rotin, D. A. (1998) *Mol. Cell. Biol.* **18,** 2608–2616
49. Blanchetot, C., and den Hertog, J. (2000) *J. Biol. Chem.* **275,** 12446–12452
50. Blanchetot, C., Tertoolen, L. G., Overvoorde, J., and den Hertog, J. (2002) *J. Biol. Chem.* **277,** 47263–47269
51. Feiken, E., van Etten, I., Gebbink, M. F., Moolenaar, W. H., and Zondag, G. C. (2000) *J. Biol. Chem.* **275,** 15350–15356
52. Debant, A., Serra-Pages, C., Seipel, K., O'Brien, S., Tang, M., Park, S. H., and Streuli, M. (1996) *Proc. Natl. Acad. Sci. U. S. A.* **93,** 5466–5471
53. Serra-Pages, C., Medley, Q. G., Tang, M., Hart, A., and Streuli, M. (1998) *J. Biol. Chem.* **273,** 15611–15620
54. Marsh, H. N., Dubreuil, C. I., Quevedo, C., Lee, A., Majdan, M., Walsh, G. S., Hausdorff, S., Said, F. A., Zoueva, O., Kozlowski, M., Siminovitch, K., Neel, B. G., Miller, F. D., and Kaplan, D. R. (2003) *J. Cell Biol.* **163,** 999–1010
55. Klesse, L. J., Meyers, K. A., Marshall, C. J., and Parada, L. F. (1999) *Oncogene* **18,** 2055–2068
56. Vaudry, D., Stork, P. J., Lazarovici, P., and Eiden, L. E. (2002) *Science* **296,** 1648–1649
57. Castellon, R., and Mirkin, B. L. (2003) *J. Neurosci. Res.* **72,** 239–249